Surface acoustic waves in two-dimensional phononic crystals: Dispersion relation and the eigenfield distribution of surface modes

Degang Zhao, Zhengyou Liu,* Chunyin Qiu, Zhaojian He, Feiyan Cai, and Manzhu Ke
Key Laboratory of Acoustic and Photonic Materials and Devices of Ministry of Education and Department of Physics, Wuhan University, Wuhan 430072, China
(Received 25 May 2007; revised manuscript received 16 August 2007; published 3 October 2007)

In this paper, we have demonstrated the existence of surface acoustic waves in two-dimensional phononic crystals with fluid matrix, which is composed of a square array of steel cylinders put in air background. By using the supercell method, we investigate the dispersion relation and the eigenfield distribution of surface modes. Surface waves can be easily excited at the surface of a finite size phononic crystal by line source or Gaussian beam placed in or launched from the background medium, and they propagate along the surface with the form of "beat." Taking advantage of these surface modes, we can obtain a highly directional emission wave beam by introducing an appropriate corrugation layer on the surface of a waveguide exit.

DOI: 10.1103/PhysRevB.76.144301 PACS number(s): 63.20.−e, 43.35.+d, 61.10.Dp, 43.20.+g

I. INTRODUCTION

The last decade has witnessed an increasing interest for the propagation of classical waves in periodic structures; typical is the propagation of electromagnetic waves in photonic crystals.[1–3] For the artificial crystals, both theory[1–3] and experiment[1] have demonstrated the existence of frequency gaps for electromagnetic waves, which forecasts potential applications of photonic crystal as optical devices.[4–7] These studies were soon extended to the propagation of elastic waves in similar periodic structures composed of materials with different elastic properties, which are known as phononic crystals (PCs).[8–19] Because of the vectorial characters of the elastic waves and the possible coupling between longitudinal and transverse modes, richer physics is expected to exist in elastic waves propagating in PCs. On the theory side, one can calculate the frequency band structure or the dispersion relations for PC,[8,9] as well as the reflection and transmission coefficients of elastic waves through a slab of a PC.[10] Generally, the PC has a macroscopic inhomogeneity, which allows a comparatively easy fabrication of the sample and a direct measurement with the widely used ultrasonic technique.[11–13] Extensive applications of PCs have also been anticipated, for example, the band gap used in sound insulations and defect states used in acoustic filters, waveguides, and so on. Recently, a refractive acoustic device by taking advantage of the features of the passband has been experimentally realized,[14] and flat acoustic lens governed by negative refraction has also been reported.[15,16]

Surface waves (SWs) in photonic crystal have been widely discussed both theoretically[17–19] and experimentally.[20] Such surface electromagnetic waves are not the result of negative dielectric constant in the metal but due to the multiple-scattering effects by dielectric scatters. They can exist in truncated photonic crystal with the surface terminated by incomplete as well as complete cells. The style of truncation strongly affects the dispersion relation and field confinement of SW for both TE and TM modes.[18] The analogy between photons and phonons aroused the research of surface elastic waves in PCs. It has been shown that surface elastic waves can be supported in semi-infinite two-dimensional (2D) solid-solid PCs, with truncated plane being parallel as well as perpendicular to the axis of periodicity.[21–23] Actually, as long as there exists a crystal-vacuum boundary, under proper conditions, the surface elastic modes will surely exist.[24] The shear module of the solid background medium of PCs plays an important role. In this paper, we choose a different PC which has a fluid background, only considering that the surface plane parallels to a row of cylinders. We use the supercell method[18,21] to study the dispersion curve and distribution of the displacement eigenfield of SW. According to the dispersion relation, we employ point source and Gaussian beam to excite SW at a finite size PC's surface and present detailed analysis to their oscillation style. For the application of SW, we introduce a waveguide structure and add an appropriate corrugation layer on its exit surface. This surface indentation modulates SW and makes them radiate into free space, then subsequently forms a highly directional wave beam.

II. SURFACE MODES' DISPERSION RELATION AND EIGENFIELD DISTRIBUTION

Our 2D PC is constituted by a square array of parallel steel cylinders (mass density $\rho=7.67\times10^3$ kg/m^3, longitudinal wave velocity $c_l=6.01\times10^3$ m/s, transverse wave velocity $c_t=3.23\times10^3$ m/s) put in air background (mass density $\rho=1.29$ kg/m^3, longitudinal wave velocity $c_l=0.34\times10^3$ m/s), with $R=0.49a$, where R is the radius of steel cylinder and a is the lattice constant. Because of the very high acoustic impedance contrast of these two components and very large filling ratio, the bulk PC can produce very wide band gaps to support the SW. We use the supercell method in conjunction with the multiple-scattering theory to study the dispersion relation and eigenfield distribution of SW. The key point of the supercell method is to design an appropriate auxiliary infinite periodic superstructure in order to apply the Bloch theorem. Figure 1 is the schematic picture of this 2D supercell, which is shown in the line frame and has length $L=23a$ and width $d=a$. This is a rectangular symmetric cell containing 11 inner cylinders. The auxiliary superstructure is formed by the infinite periodic translation of

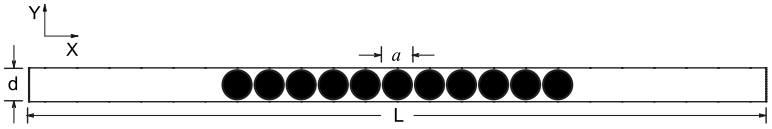

FIG. 1. A supercell shown in the line frame. The sample is composed of steel cylinders with radius $R=0.49a$ put in air background. The lengths of crystal slab and air slab are $11a$ and $12a$, respectively. The supercell has length $L=23a$ and width $d=a$. It is homogeneous along the z direction.

the unit cell, i.e., the supercell, along both x and y axes. It is constituted by crystal slabs with width $11a$ alternating with air slabs with width $12a$. It is a suitable sample that the crystal slab and air slab are both thick enough to ensure that the surface modes at any two neighboring crystal-air interfaces do not interact with each other. Under this limit, the dispersion curve obtained is expected to converge to the dispersion curve of the surface modes of the semi-infinite crystal.

Firstly, we present the bulk band structure of a periodic square array of steel cylinders with radius $R=0.49a$ put in air background in Fig. 2(a). As can be seen, the PC generates a complete band gap in the reduced frequency (hereafter, all the involved frequencies are reduced by $2\pi c/a$, where c is the longitudinal wave velocity in air) ranging from about 0.25 to 0.95. This gap is wide enough and its lower edge appears in the very low frequency of 0.25; therefore, the sample is a good candidate to support surface modes.

As is known, SW is characterized by the decaying field on both sides in perpendicular directions away from the surface plane. For our system, on the air side, the exponential decay of the field is a straightforward consequence of the propagation vector along the surface being greater than the background wave vector, whereas on the crystal side, the field decays because of Bragg scattering effects in band gaps. That is to say, the dispersion curves of SW must satisfy two essential conditions: be restricted to the right side of the background dispersion line and lie within the band gaps of the bulk crystal. Figure 2(b) shows the dispersion curves of SW (solid line) mixed with the projected bands on the Γ-X direction (shaded region) and the background dispersion line (dashed line). It clearly shows that the surface modes appear close to the first Brillouin zone boundary, in a narrow frequency range from about 0.4 to 0.46, and the curve emanates from the dispersion line of the background. There is a simple physical picture for the surface mode. The outmost periodically arrayed cylinders (i.e., the surface) of the PC Bragg scatter the acoustic wave propagating parallel to the surface, making the background dispersion line curve downward, which results in the enlarging of the wave number corresponding to a frequency, such that the acoustic waves become attenuated along the normal on the background side, while on the PC side, they attenuate because of the gap. Hence, the scattering of the surface structure to acoustic waves plays an important role in the creation of the surface mode. The bigger the cylinder size (i.e., the higher the filling fraction), the stronger the scattering, and consequently the bigger the deviation of the dispersion curve from the air line and the easier a surface mode to be observed. In other words, the dispersion curve of the surface mode is continuously dependent on the filling fraction. For very high filling fraction (as the case discussed here, $R/a=0.49$, there is a big deviation of the dispersion curve from the background dispersion line, in case the surface mode has a short attenuation length so that the surface mode is easier to demonstrate, while for lower filling fraction (e.g., $R/a=0.3$ or 0.4), the dispersion curve is closer to the background line from below, in case the surface mode has a comparatively longer attenuation length.

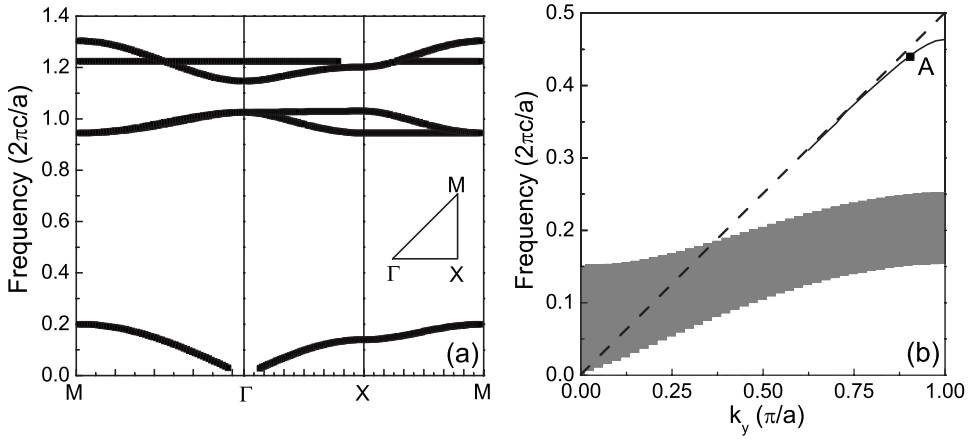

FIG. 2. (a) Bulk band structure for the PC consisting of steel cylinders put in air background with a square lattice. The radius of cylinder is $R=0.49a$. Inset is the irreducible Brillouin zone. (b) Surface mode dispersion curves (solid line) in the first band gap. Dashed line is the dispersion line of air background. Shaded region is the projected bulk bands on the Γ-X direction. k_y is the wave vector along the crystal-air interface, in unit of π/a. The frequencies of both two pictures are in unit of $2\pi c/a$, where c is the longitudinal wave velocity in air.

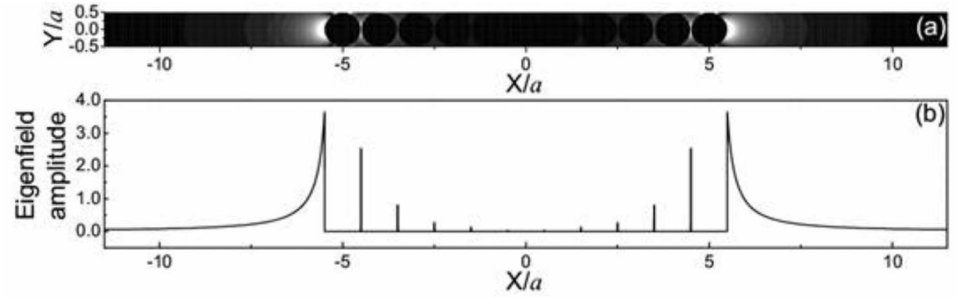

FIG. 3. (a) Spatial distribution of displacement eigenfield in a supercell for mode *A*. Lightness and darkness denote strong and weak intensities, respectively. (b) Extractive field at the $y=0$ axis of Fig. 3(a).

For even lower filling fraction, the surface mode approaches the bulk mode with an even longer attenuation length, in case the dispersion curve incorporates into the background line, which means the disappearance of the surface mode.

For further analysis of surface modes, we investigate the eigenfield distribution of mode *A* [marked in Fig. 2(b)], which has wave vector $k_y=0.9\pi/a$ and frequency $\omega=0.44$. Figure 3(a) displays the spatial distribution of the displacement eigenfield amplitude in a supercell for mode *A*. In order to observe the variation of field more clearly, we extract numerical values of Fig. 3(a) at the $y=0$ axis in Fig. 3(b). The eigenfield distribution is centrosymmetric and the strongest field value is localized at the crystal-air interfaces. In air slab, away from the surface, the field amplitude rapidly decays as an exponential function, which is like a Rayleigh surface wave. In crystal slab, the field only exists in the interspaces between cylinders and also declines when close to the center of the supercell. The field amplitude of the inner cylinder remains zero because compared with air background, steel is like a rigid medium and acoustic waves are almost totally reflected on the interfaces.

III. SURFACE ACOUSTIC WAVES AT FINITE SIZE SURFACE

From Fig. 3, we can find that the field amplitude closely approaches zero at the boundary and at the center of a supercell, that is to say, the air slab and the crystal slab which we choose are both thick enough to prevent the coupling of the surface modes at every two neighboring crystal-air interfaces. So when the supercell becomes bigger, the surface modes will keep steady. Extremely when the air slab in a supercell broadens without limit, only leaving a single crystal slab in air background, it is anticipated that the surface modes can still survive. However, it is impossible to calculate eigenmodes for infinite supercell, so we need an external source to excite surface acoustic waves. We select a finite size PC, which has width $7a$ and length $60a$, placed in air background and discuss how to excite SW at its surface. To our knowledge, if a source can offer big angle incident waves on the surface, the SW will be easily excited. We perform a numerical simulation for using line source (parallel to the z direction) and Gaussian beam (homogeneous in z direction) to induce SW, and the structure is graphically shown in Fig. 4(a). Firstly, let us consider the point source, which is placed at $S(x=0,y=0)$, holding a distance a above the crystal-air surface. The incident frequency is 0.44, matching mode *A*. The near-field spatial distributions of pressure field are plotted in Fig. 4(b). We can see that the energy radiated from the source is separated into two parts: one spreads upward in all directions, maintaining configuration of a point source, whereas the other is localized at the surface, taking nonradiative surface modes. Next, we take account of the Gaussian beam, which has an incident angle of 70° and also holds a frequency of 0.44. The radiated field, plotted in Fig. 4(c), has also been divided into two parts: one is reflected at the surface as the reflected angle equals the incident angle, and the other is SW propagating along the surface. Actually, except the amplitude and original phase, the configurations of SW induced by these two different sources are absolutely the same (detailed analysis is presented later). It can also be clearly observed that these sur-

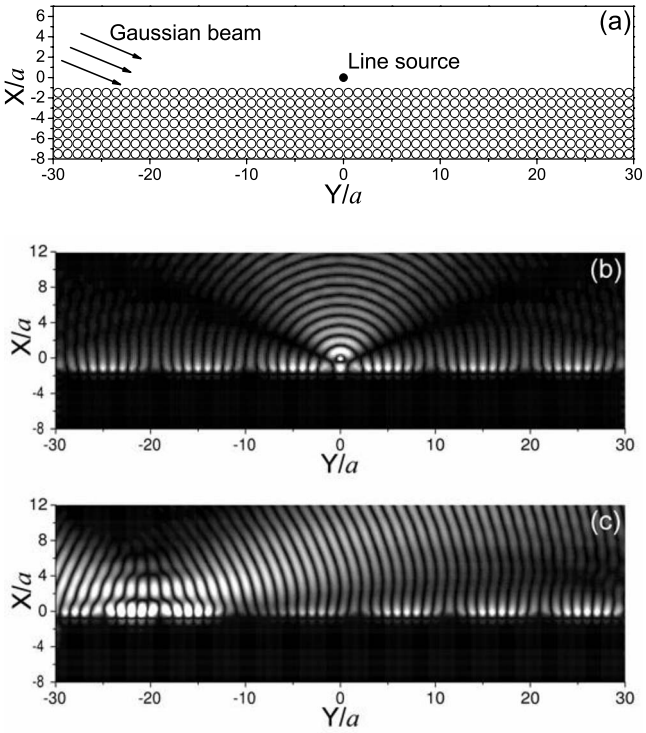

FIG. 4. (a) Schematic picture of structure and external sources for inducing SW. Line source is placed at $S(x,y=0)$ parallel to the z direction, holding distance a above the surface. Gaussian beam has the incident angle of 70°. The incident frequency of both sources is 0.44. (b) Near-field spatial distribution of pressure field generated by the line source. (c) Near-field spatial distribution of pressure field generated by the Gaussian beam.

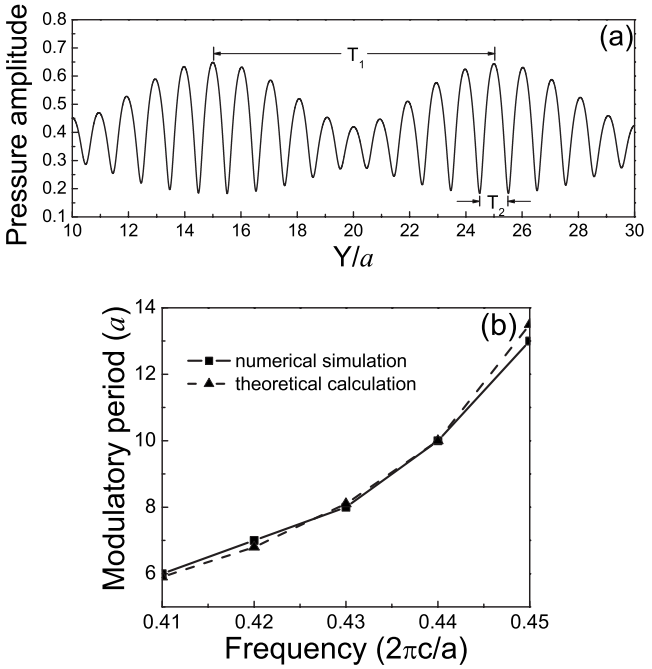

FIG. 5. (a) Extractive field amplitude value along the surface in the range from $10a$ to $30a$ on the y axis of Fig. 4(b). (b) Dependence of modulation period of "beat" versus incident frequency. Solid line is the result of numerical simulation and dashed line is the result of theoretical calculation.

face modes rapidly attenuate to zero in the x direction away from the surface.

It needs to point out that the preceding discussions in Sec. II about SW's dispersion relation and eigenfield distribution are for infinite system. Theoretically, SW cannot be excited by any source placed in background medium when the surface has an infinite length. Because from Fig. 2(b), in the same frequency, the background wave vector is always smaller than the wave vector of SW. However, for finite size surface, for a given frequency, the permissive SW's wave vector is no longer a single certain value k but has an oscillatory range Δk, which satisfies the relation $\Delta y \Delta k \sim 1$, where Δy approximates the measure of the length of surface. As long as Δy is not particularly big, wave vector from external sources can always fall in the Δk range, then the SW will be certainly excited. So, we can infer that the SW is the inherent property for our system. It has nothing to do with the type and the location of source but only depends on the incident frequency.

We extract a part of field amplitude value of Fig. 4(b) [the characters of SW in Figs. 4(b) and 4(c) are the same, so we only need to choose one of them] along the surface to investigate detailed physical properties [see Fig. 5(a), the oscillation style of the SW is a representative "beat" mode]. As is known, beat is formed by the interference of two coherent waves which keep the same propagation direction and amplitude but have little wave vector difference. The SW is a Bloch-type wave, so the wave function can be written as $\psi_k(y)=u(y)e^{iky}$, where $u(y)$ is a periodic modulation function and its period is the lattice constant a, while k is the Bloch wave vector of SW. The beat originates from the interference of two surface modes, which possess wave vectors $k_1=0.9\pi/a$ and $k_2=2\pi/a-k_1=1.1\pi/a$, respectively. Actually, they are a couple of degenerate states and symmetrically take the first Brillouin zone boundary as the symmetrical center. Thus, the modulatory period of beat is $T_1=2\pi/(k_2-k_1)=10a$. We solve the modulation period in different SW's frequencies by both numerical simulation and theoretical calculation and compare them to check this beat effect. In Fig. 5(b), it is clearly found that they match very well. In the wave package, the small vibrational period $T_2=a$ originates from the periodic function $u(y)$.

IV. COLLIMATION EFFECT

In recent years, some research has been done to achieve highly directional emission of light beam via utilizing surface electromagnetic waves in a waveguide structure.[25,26] They firstly decrease the radius of the surface monolayer cylinders at both sides of the waveguide exit to induce surface states. Then, they made some appropriate corrugation on that monolayer, which provided a periodic modulation to the surface electromagnetic waves. This surface modulation can produce a collimated light beam. However, using surface acoustic waves to achieve collimation effect has not been reported. We did this work and for our system, the problem is much simpler because the surface acoustic waves have already been induced easily. So long as analogously design a waveguide structure and do some appropriate corrugation on its exit surface, we can also engineer beaming effect.

Figure 6(a) shows the considered waveguide structure, which has no surface corrugation. A bulk of finite size PC, of length $40a$ and width $7a$, is placed in air background and a row of cylinders along the plane $y=0$ are removed to construct a waveguide. Figure 6(b) is the near-field spatial distribution of pressure field radiated from a line source placed at the waveguide entrance $S(x=0,y=0)$ and the emissive frequency is also chosen as 0.44. Above all, the frequency 0.44 falls into the absolute band gap of the bulk PC, that is to say, it can support a waveguide mode. So, the propagation of radiative waves from the source is restricted in the waveguide and cannot penetrate into the PC, whereas at the entrance and exit of the waveguide, since there is no restriction, waves diffract in all directions like a point source. On the other hand, a frequency of 0.44 lies within the range of SW's frequency, so the source will excite SWs at both upper and lower surfaces. Figure 6(b) clearly shows that the propagation of surface mode along the surface still takes the form of beat, which is similar to Figs. 4(b) and 4(c). Under this condition, the waveguide mode and the surface mode are independent, and there is no interaction. So, in order to produce a directional beam, it needs to introduce some modulation to the surface mode and make it couple with the waveguide mode. A simple scheme is to add a number of steel cylinders on each side (the left and the right) surface of the waveguide exit to form a corrugation layer, which has a smaller radius $r=0.4a$, as schematically shown in Fig. 6(c). Here, the number of cylinders on each side surface of the exit (denoted with N) is $N=10$. On the x axis, they are placed at the $x=7a$ plane, $0.5a$ above the surface. On the y axis,

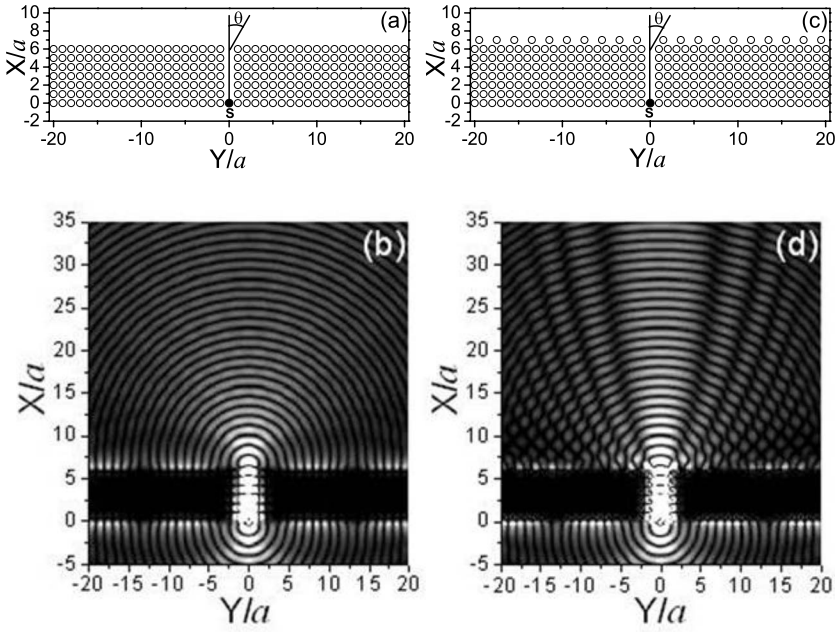

FIG. 6. [(a) and (c)] Schematic pictures of waveguide structure without and with modified surface, respectively. The point source with frequency of 0.44 is placed at $S(x=0,y=0)$ [see text for more detailed description of the corrugation layer for Fig. 6(c)]. θ is the azimuthal angle. [(b) and (d)] Near-field spatial distribution of pressure field for (a) and (c), respectively.

they are periodically (period $T_c=2a$) placed at $y=\pm 1.5a, \pm 3.5a, \pm 5.5a, \ldots$; namely, these cylinders are placed above on the middle of two bulk crystal cylinders. Since only one layer of sparse corrugation is introduced, there would be only a slight modification to the dispersion of the surface mode. However, this modification can make the surface mode leaky or radiative, while it maintains the overall surface mode feature (e.g., the energy flux dominantly confined around the surface). Spatial distribution of the near-field pressure field for this modified structure is plotted in Fig. 6(d). Compared with Fig. 6(b), because of the modulation to surface modes, the nonradiative SW along the upper surface is transferred into the radiative mode. As a result, the wave diffracted by the waveguide exit couples with the modulated SW and they constructively interfere with each other at the center. Then, directional beam radiating upward along the x direction with very little angle divergence can be distinctly observed.

The corrugation layer resembles a diffraction grating illuminated by SW. Beaming effect is expected when the grating period T_c coincides with the surface modes' modal wavelength λ_s. The SW at the surface holds the beat mode; hence, the average wave vector is $k_s=(k_1+k_2)/2=\pi/a$, so the modal wavelength is $\lambda_s=2\pi/k_s=2a$, which exactly equals T_c. A reciprocal lattice vector $k_h=2\pi/T_c=\pi/a$ is added to the SW's wave vector, folding the mode dispersion relation into the core of Brillouin zone; namely, the nonradiative surface mode is transferred into the radiative mode. Then, all the diffracted waves interfere in free space, giving rise to the zero-level main maximum in the center of diffraction grating, which is presented as a highly directional beam in far field.

The collimation quality can be judged by the far-field divergence angle θ, which depends on many momenta of corrugation. Fixing the location of corrugation scatterers, we draw the far-field pressure field amplitude as a function of θ for different radii and for different numbers of corrugation layer cylinders in Figs. 7(a) and 7(b), respectively. In Fig. 7(a), when there is no corrugation, the curve is a fluctuant line, i.e., acoustic waves spread in all directions and no collimation effect, which matches Fig. 6(b). Only when corrugation has been done on the surface the beaming phenomenon arises. The corrugation layer cylinders' radius greatly affects the collimation quality. When the radius is small, SW cannot feel the change of surface and the modulation is weak. As the radius increases, the central peak distinctly appears. However, that does not mean that the bigger the radius, the greater the collimation. Actually, the optimized radius is $r=0.4a$, and when the radius rises to the biggest value

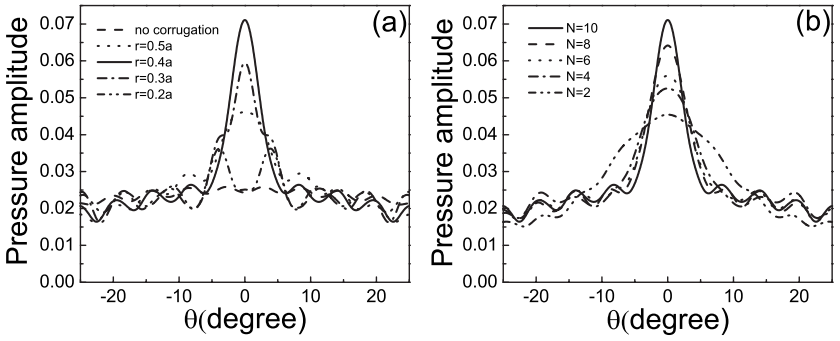

FIG. 7. Far-field radial component of pressure field amplitude radiated out of modified waveguide exit as a function of azimuthal angle θ for (a) different radii (r) and (b) different numbers (N) of corrugation layer cylinders, respectively

$r=0.5a$, the peak value at the center is lower than the optimization because of the strong reflection by the big cylinders. The number of cylinders in the corrugation layer (described with N, the number of cylinders on the left or right side surface of the exit, located at the places with $y=\pm 1.5a, \pm 3.5a, \pm 5.5a\ldots$, beginning from $y=\pm 1.5a$; for the system shown in Fig. 6(b), $N \leqslant 10$] is also an important factor. From Fig. 7(b), we can find that the more the cylinders, the more energy is collected to converge in a narrower angle at the center. This character is the same as a diffraction grating: the increasing of the number of grating slits causes the narrowing of the interference maxima. So, the optimized number is $N=10$. Under optimum conditions, the far-field divergence angle is only about 6.0°.

V. CONCLUSION

In this paper, we use the supercell method to investigate surface acoustic waves in 2D solid-fluid phononic crystal, which is composed of square array of steel cylinders put in air background with high filling fraction $R/a=0.49$. The surface modes appear within a narrow frequency range near the first Brillouin zone boundary, from about 0.4 to 0.46. The eigenfield distribution of a certain surface mode distinctly exhibits the SW's basic character: decays in perpendicular directions at both sides away from the surface plane. Next, we concentrate on SW at a finite size PC's surface. The SW can be easily excited by external sources placed in background medium, and its configuration is the representative beat mode, which is formed by the interference of two Bloch waves having wave vectors $k_1=k$ and $k_2=2\pi/a-k$, respectively. It possesses both modulatory period $T_1=2\pi/(k_2-k_1)$ and vibrational period $T_2=a$. For further application of SW, we introduce a waveguide structure and make corrugation on the surface at both sides of the waveguide exit to offer appropriate periodic modulation to the SW. This modulation changes the nonradiative SW into radiative waves, which constructively interfere at the center of waveguide and subsequently generate a collimated beam emitting along one direction with little angle divergence in far field. The collimation quality depends on many factors, and under optimized conditions, the far-field divergence angle is only about 6.0°. The surface acoustic wave beaming effect may have important application in ultrasonic device designing.

ACKNOWLEDGMENTS

This work was supported by the National Natural Science Foundation of China (Grants Nos. 50425206 and 10418014).

*Author to whom correspondence should be addressed; zyliu@whu.edu.cn

[1] E. Yablonovitch, Phys. Rev. Lett. **58**, 2059 (1987); E. Yablonovitch and T. J. Gmitter, *ibid.* **63**, 195 (1989).
[2] K. M. Ho, C. T. Chan, and C. M. Soukoulis, Phys. Rev. Lett. **65**, 3152 (1990); C. T. Chan, K. M. Ho, and C. M. Soukoulis, Europhys. Lett. **16**, 563 (1991).
[3] X. D. Wang, X. G. Zhang, Q. Yu, and B. N. Harmon, Phys. Rev. B **47**, 4161 (1993).
[4] M. Loncar, D. Nedeljkovic, T. Doll, J. Vuckovic, A. Scherer, and T. P. Pearsall, Appl. Phys. Lett. **77**, 1937 (2000).
[5] S. Noda, A. Chutinan, and M. Imada, Nature (London) **407**, 608 (2000).
[6] S. Y. Lin, E. Chow, J. Bur, S. G. Johnson, and J. D. Joannopoulos, Opt. Lett. **27**, 1400 (2002).
[7] A. Martinez, F. Cuesta, A. Griol, D. Mira, J. Garcia, P. Sanchis, R. Llorente, and J. Marti, Appl. Phys. Lett. **83**, 3033 (2003).
[8] M. S. Kushwaha, P. Halevi, M. Martinez, L. Dobrzynski, and B. Djafari-Rouhani, Phys. Rev. B **49**, 2313 (1994).
[9] J. Mei, Z. Liu, J. Shi, and D. Tian, Phys. Rev. B **67**, 245107 (2003).
[10] I. E. Psarobas, N. Stefanou, and A. Modinos, Phys. Rev. B **62**, 278 (2000).
[11] F. R. Montero de Espinosa, E. Jimenez, and M. Torres, Phys. Rev. Lett. **80**, 1208 (1998).
[12] J. O. Vasseur, P. A. Deymier, B. Chenni, B. Djafari-Rouhani, L. Dobrzynski, and D. Prevost, Phys. Rev. Lett. **86**, 3012 (2001).
[13] A. Khelif, A. Choujaa, S. Benchabane, B. Djafari-Rouhani, and V. Laude, Appl. Phys. Lett. **84**, 4400 (2004).
[14] F. Cervera, L. Sanchis, J. V. Sanchez-Perez, R. Martinez-Sala, C. Rubio, F. Meseguer, C. Lopez, D. Caballero, and J. Sanchez-Dehesa, Phys. Rev. Lett. **88**, 023902 (2001).
[15] X. D. Zhang and Z. Y. Liu, Appl. Phys. Lett. **85**, 341 (2004).
[16] C. Y. Qiu, X. D. Zhang, and Z. Y. Liu, Phys. Rev. B **71**, 054302 (2005).
[17] R. D. Meade, K. D. Brommer, A. M. Rappe, and J. D. Joannopoulos, Phys. Rev. B **44**, 10961 (1991).
[18] F. Ramos-Mendieta and P. Halevi, Phys. Rev. B **59**, 15112 (1999); , J. Opt. Soc. Am. B **14**, 370 (1997).
[19] S. Enoch, E. Popov, and N. Bonod, Phys. Rev. B **72**, 155101 (2005).
[20] W. M. Robertson and M. S. May, Appl. Phys. Lett. **74**, 1800 (1999).
[21] B. Manzanares-Martínez and F. Ramos-Mendieta, Phys. Rev. B **68**, 134303 (2003).
[22] Elena V. Tartakovskaya, Phys. Rev. B **62**, 11225 (2000).
[23] Yukihiro Tanaka and Shin-ichiro Tamura, Phys. Rev. B **58**, 7958 (1998).
[24] M. Torres, F. R. Montero de Espinosa, D. García-Pablos, and N. García, Phys. Rev. Lett. **82**, 3054 (1999).
[25] Esteban Moreno, F. J. Garcia-Vidal, and L. Martín-Moreno, Phys. Rev. B **69**, 121402(R) (2004).
[26] Steven K. Morrison and Yuri S. Kivshar, Appl. Phys. Lett. **86**, 081110 (2005).